Optimization of Forced-Air Cooling System for Accurate Design of Power Converters

A. Castelan[1], B. Cougo[1], J. Brandelero[2], D. Flumian[2], T. Meynard[2]
[1] : Institute of Technological Research Saint-Exupery, IRT Saint-Exupery, Toulouse, France
anne.castelan@irt-saintexupery.com
2 : Laboratory of Plasma and Energy Conversion, LAPLACE, Toulouse, France
brandelero@laplace.univ-tlse.fr

***Abstract*— Finding a global optimum of power converters requires models of all its parts (semiconductors, filters and cooling system), rules to describe the interactions between the different parts, an optimality criterion and optimization routines to converge towards the best design. In this paper we implement a model of forced-air cooling system to be used in such a design process. Heat exchange between fins and forced air is described, and fluid mechanics are used to account for the interactions between the fan and the heat sink. Using these descriptions, it is shown how a given performance index can be maximized using optimization routines. The developed model is experimentally verified in the case of a custom heat sink designed with this process. Finally, we investigate the influence of different parameters such as the fan power and characteristic, base plate, heat sink dimensions and materials.**

Keywords—Heat sink optimization, Forced-air cooling, Power converter

I. INTRODUCTION

With the development of embedded systems, power electronics has to adapt and go further in terms of integration for a final objective of reducing weight and volume of equipment while maintaining a good performance.

The optimal design can be aided by using optimization routines that will vary the parameters describing the different objects until an optimality criterion is met [1,2]. This requires models to predict the evolution of each part and a description of the interactions between all parts to make sure that design constraints are met. Describing the full physics inside a converter and running optimization routines using such a detailed description seems impossible, but in this first section, we will show that very simple models already give a good understanding of the main interactions in a power converter.

As an example, we will show here that it is possible to obtain a quite realistic estimate of the evolution of the total weight and losses of a converter as a function of the switching frequency by means of extremely simple models.

Let's consider, first, that the capacitors have no losses and that their weight can be expressed as:

$$weight_C = k_1 C.V^2 \qquad (1)$$

With k_1 a proportionality coefficient, C the value of the capacitance, and V the maximum voltage across the capacitor. Then we will assume that the weight of inductors is like:

$$weight_L = k_2.L.I_{peak}.\ I_{RMS} \qquad (2)$$

And their losses given by:

$$losses_L = k_3.weight_L. \qquad (3)$$

We will also say that heat sinks generate no losses but their weight is given by:

$$weight_{HS} = k_4/R_{th}. \qquad (4)$$

Finally, a semiconductor can be considered without any weight but with losses such as:

$$losses_{SC} = P_{Conduction} + E_{switching}.F_{switching}. \qquad (5)$$

With equations (1) to (5) inserted in a simple Excel sheet, we can generate curves (see Fig. 1) representing the evolution of the weight and losses of a converter with the specifications shown in Table I.

PARAMETERS OF GENERIC POWER ELECTRONIC SYSTEM

V_{in}	100V
I_{out}	10A
$\Delta\theta$	50°C

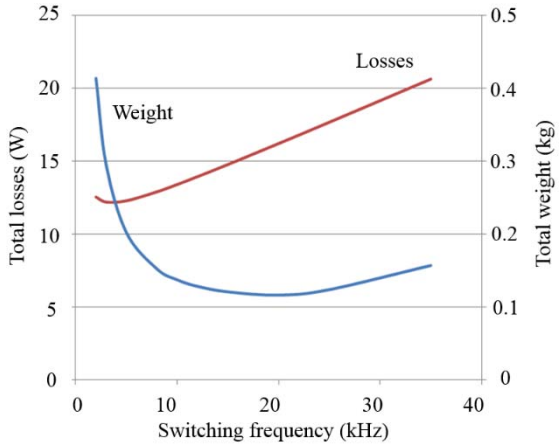

Evolution of weight and losses of a 1kW converter vs switching frequency.

With this kind of model, we can observe that there is an optimum for efficiency at a very low switching frequency (3kHz), the losses being dominated by the losses in the inductor under this point and by the losses in the semiconductor above this point. The optimal weight is reached at around 20kHz, with bulky filters under this frequency and bigger heat sinks above this frequency. This behavior is quite typical of power electronics converters, and we can see that it is represented here via few basic relations only. Obviously, depending on the technology, factors k_1 to k_4, $P_{conduction}$ and $E_{switching}$ need to be adapted and the optimal points can significantly change. It is the purpose of this paper to improve the accuracy of the models used and to utilize more adapted tools to create and process these new models.

It can be seen that in order to allow optimization of static converters we need to build models with different levels of precision for all the components of a converter. These models are described as “objects” and they all use the same architecture: the entries are physical data such as shape, dimensions and materials. Then the “object” includes some properties describing its physic. The outputs will be the weight, volume, losses, cost or any other useful information. Three levels of precision are available to answer different requirements in terms of speed/accuracy trade-off.

Previous works have already been made for inductors, capacitors and semiconductors [3][1]. This paper concentrates on a cooling system composed of heat sink and fan, but the aim is definitely to use it altogether with the other models to run optimization routines at the converter level. This article will be focused on a plate+fin heat sink. Cooling system will be modeled and we will compare the results obtained with MATLAB routines and the measurements on an experimental setup.

II. Cooling System Modeling

A forced-air cooling system is composed mainly of a fan and a heat sink. Both of them represent an important part on the final weight and thermal resistance and both of them must be accurately modeled.

A. Fan modeling

In [4] authors propose a continuous model of the fan volume depending on the airflow and pressure. In this paper, fans are considered as discrete objects for the cooling system optimization. They are characterized by the mass, power, supply voltage, physical characteristics such as the diameter and thickness and hydraulic quantities such as pressure and volumetric air flow (Fig. 2). Air speed of the fan depends on the heat sink attached to the fan.

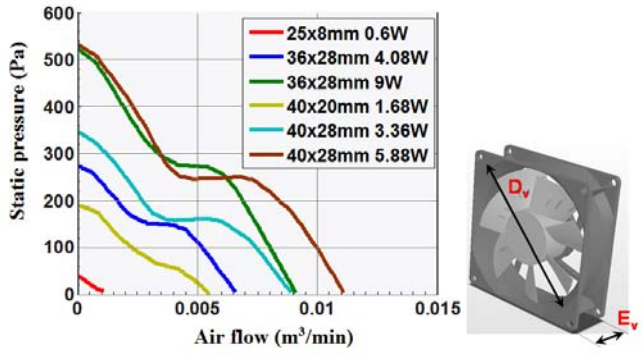

Fig. 1. Hydraulic characteristics of different axial fans having different power and dimensions.

B. Heatsink modeling

Extruded heat sink, shown in Fig. 3, is defined by different dimensions such as its length L, by the fin thickness E_a, the space between two fins b, by the fin height H_a, the base plate height H_p and by the number of fins N_{ba}. As a result, the geometry of a heat sink is fixed, total heat sink width; height and weight (given the material density) are calculated on the basis of these parameters. The procedure for determining the thermal resistance is close to that of [5] and will be explained below. Experimental validation of this model will be given in Section III.

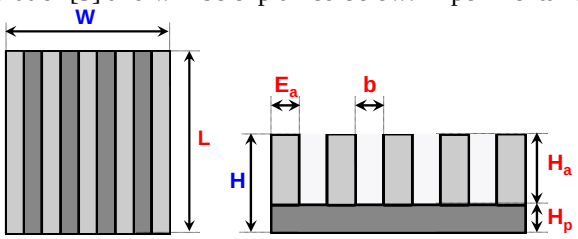

Fig. 2. Extruded heatsink dimensions; a) top view; b) front view.

Hydraulic and thermal problems are solved using three normalized parameters:

Prandtl number Pr (fluid characteristics)

Reynolds number Re (normalized fluid flow)

Nusselt number Nu (normalized heat transfer by convection).

$$Pr = \frac{\mu \cdot c_p}{\lambda_{fluid}} \tag{6}$$

With c_p the fluid specific heat at a constant pressure and λ_{fluid} the fluid thermal conductivity

$$Re = \frac{\rho \cdot v \cdot b}{\mu} \tag{7}$$

Equation *(8)* express the Reynolds number changed by a multiplied term b/L.

$$Re^* = \frac{\rho \cdot v \cdot b}{\mu} \cdot \frac{b}{L} \tag{8}$$

With ρ the fluid density, v the mean fluid speed and μ the fluid dynamic viscosity

Equation *(9)* brings a formulation of the Nusselt number given by authors of [6]. It's a formulation based on a heat transfer mixed model, deducted by comparing numerical simulations on a Reynolds number variation range between $0.1<Re^*<100$.

$$Nu = \left(\frac{1}{\left(\frac{Re^* \cdot Pr}{2}\right)^3} + \frac{1}{\left(0.664 \cdot \sqrt[3]{Pr} \cdot \sqrt{Re^* + 3.65 \cdot \sqrt{Re^*}}\right)^3} \right)^{-1/3} \tag{9}$$

Thermal resistance

Heat sink thermal resistance is given by the conduction resistor of the plate, the conduction resistor of fins and the convection resistor of the fins and the air circulating between fins. The equivalent circuit of heat sink model is shown Fig. 4.

The thermal resistance of the base plate R_{base} (10) does not model the 2D effects which exist when there are several heat sources. Obviously, any optimization not taking this 2D effect into account will result in a base plate having a height H_p equal to zero, in order to minimize R_{base} and the heat sink weight. Here we consider a base plate having a fixed height of 8mm, which is enough for mechanically attach most of medium and low power semiconductors on standard packaging. Optimization of this base plate height will be addressed in the future.

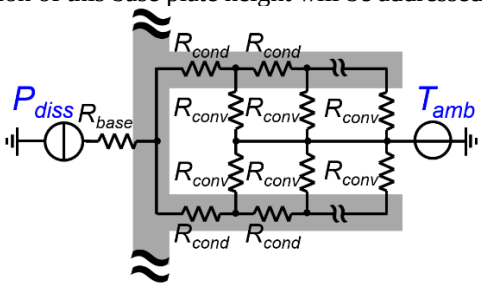

Fig. 3. Modeling of the fins temperature gradient effects by a network of y thermal resistance modules.

$$R_{base} = \frac{H_p}{\lambda_{base} \cdot W \cdot L} \tag{10}$$

With λ_{base} the base plate material thermal conductivity. Contrarily to many different references [4,5], the temperature gradient effect which exists along the fins has been taken account by a network of y modules composed of a R_{cond} resistance *(11)* parallel to a R_{conv} resistance *(12)*

$$R_{cond} = \frac{1}{y} \cdot \frac{H_a}{\lambda_{fin} \cdot E_a \cdot L} \quad (11)$$

$$R_{conv} = \frac{1}{y} \cdot \frac{1}{h \cdot A_{fin} \cdot \eta_{fin}} \quad (12)$$

With h the heat transfer coefficient *(13)*, A_{fin} the surface of the side of each fin and η_{fin} the fin efficiency defined by *(14)*

$$h = Nu_b \cdot \frac{\lambda_{fluid}}{b} \quad (13)$$

With Nu_b the Nusselt number *(9)* and λ_{fluid} the thermal conductivity of the fluid between fins.

$$\eta_{fin} = \frac{\tanh\left(\sqrt{\frac{2.h}{\lambda_{fin} \cdot E_a}} \cdot H_a\right) \cdot \sqrt{\lambda_{fin} \cdot E_a}}{H_a \cdot \sqrt{2 \cdot h}} \quad (14)$$

With λ_{fin} the fin thermal conductivity, E_a and H_a are respectively the thickness and the height of a fin.

The equivalent resistance of a fin, function of the number of modules y, is given by

$$R_{fin} = -\frac{1}{2} \cdot \frac{A.(-B^y) - R_{cond} \cdot (-B)^y + A \cdot C^y + R_{cond}}{(-B)^y - C^y} \quad (15)$$

$$A = \sqrt{R_{cond} \cdot (R_{cond} + 4 \cdot R_{conv})}$$

$$B = \frac{\sqrt{-2 \cdot R_{conv} - R_{cond} + A}}{R_{conv}}$$

$$C = \frac{2 \cdot R_{conv} + R_{cond} + A}{R_{conv}}$$

Modeling the fin resistance by a resistance network can significantly increase the accuracy of the heat sink thermal resistance calculation as it will be shown in Section III, especially for thin fins, which is usually the case of optimized heat sinks.

Finally, the heat sink resistance is given by paralleling resistance of the fins, in series with the base plate resistance

$$R_d = R_{base} + \frac{R_{fin}}{2 \cdot Nb_a} \quad (16)$$

Average air speed

The air speed between heat sink fins *(17)* used in Reynolds equation, gives a direct relation with the volume flow rate delivered by the fan and named G.

$$v = \frac{G}{N_{ba} \cdot b \cdot H_a} \quad (17)$$

The operating point of a fan is determined with its pressure drop characteristic ΔP, by the volumetric flow rate of the fan and of the heat sink. This curve is given by the fan manufacturer (22). For the heat sink, it can be calculated with the equation *(18)*.

$$\Delta P = \frac{v^2}{2} \cdot \rho \cdot (K_c + K_e + f_{app}) \quad (18)$$

With ρ the air density, K_c and K_e losses due to sudden contraction and sudden expansion of the entry and output flow of channels between fins respectively given by *(19)* and *(20)*, f_{app} losses due to apparent friction *(21)*

$$K_c = 0.42 \cdot \left(1 - \left(1 - \frac{E_a \cdot Nb_a}{W}\right)^2\right) \quad (19)$$

$$K_e = \left(1 - \left(1 - \frac{E_a \cdot Nb_a}{W}\right)^2\right) \quad (20)$$

$$f_{app} = \frac{L}{R_e \cdot b} \cdot \sqrt{\frac{47.33 \cdot b \cdot R_e}{L} + (2 \cdot f)^2} \quad (21)$$

Where f *(22)* is a function of the ratio b/H_a, named ψ.

$$f = 24 - 32.527 \cdot \psi + 46.721 \cdot \psi^2 - 40.829 \cdot \psi^3 + 22.954 \cdot \psi^4 - 6.089 \cdot \psi^5 \quad (22)$$

III. Heatsink Optimization regarding Weight and Thermal Resistance

Using equations from *(6)* to *(22)*, one can minimize the cooling system total thermal resistance for a given heat sink volume and fan. As an example, consider a heat sinks which has a base plate of 8mm high and 40mm wide and fins with 40mm high. If we vary the number of fins N_{ba} having a thickness of 0.8mm and also the fan attached to the heat sink, we find the results shown in Fig. 5. Figure 5a) shows the hydraulic characteristics of the heat sinks with a variation of the fins number and for different fans having with different powers. Figure 5b) shows the mean air speed between fins and the thermal resistance with a variation of the number of fins.

As shown in other papers [4], we can notice that there is a number of fins which minimize the thermal resistance of the heat sink. Moreover we can see a zone where the thermal resistance increases. In this zone, uninteresting for design, the pressure drop is important, so using a powerful fan helps reducing the thermal resistance of the heat sink. In the other zone, interesting for the design, the augmentation of the fan power has a low impact on the thermal resistance.

Power converters for aircrafts, which are the main application topic treated in this paper, are usually optimized for global weight minimization and system efficiency maximization. Thus minimizing the cooling system thermal resistance for a given volume does not optimize the system. Therefore we define a performance index, called here $CSPI_M$, which can be used to compare different forced-air cooling systems. This index depends on the heat sink thermal resistance R_{hs} and the cooling system weight M_{hs} comprising the heat sink weight and the fan weight. The index is defined as:

$$CSPI_M=(R_{hs} \cdot M_{hs})^{-1} \qquad (23)$$

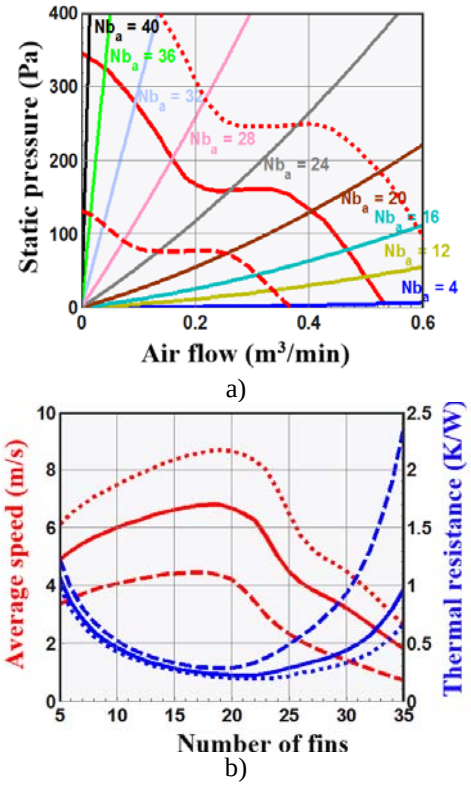

Fig. 4. Design of heat sinks with forced convection for heat sinks of same external dimensions and with different number of fins and for three different fans. a) static pressure versus air flow rate characteristic of fans and b) evolution of the mean speed between fins and the thermal resistance function of the number of fins.

A. Thermal model accuracy variation with the number of elements in the resistance network

As said before, many authors [7,8] use a single element to model the fin resistance (R_{cond}) and also a single element to model the fin/air resistance (R_{conv}). When the number of elements increases, as shown in Section II, there is a gain in accuracy. It can be observed in the example given below.

Considering a heat sink having a base plate height H_p=8mm, width and fin height W=H_a=40mm and heat sink length L=100mm, one can calculate the performance index $CSPI_M$ for different number of fins N_{ba}, different fin widths and for different number of elements in the resistance network N_r. In order to simplify the analysis, we define a fin space ratio k which represents the total thickness of all fins compared to the total heat sink width and is given below:

$$k=N_{ba} \cdot E_a/W \qquad (24)$$

Fig. 6 shows the variation of the performance index with k and number of elements in the resistance network N_r for a number of fins equal to 10 and 17. The material used for the heat sink is aluminum and the fan is a Sanyo Denki 9GA0412P3J01 40x40mm of rated power 5.9W.

Note that the smaller the k is, the thinner the fins are and consequently the higher are the difference between using one or many elements in the resistance network. Also note that this difference is high in the region where most of heat sinks are designed (k<0.4). Also, for the optimal heat sink i.e. the one with highest $CSPI_M$ (for k=0.225), the difference between the model with 1 and 10 elements is equal to about 18%. This difference is confirmed by

experimental results. We have built an extruded heat sink having the same characteristics of those considered in Fig. 6 and having a number of fins equal to17 and k=0.34 (giving a fin width of 0.8mm), which can be seen in Fig. 7. Measurements of thermal resistance give the point marked with a star in Fig. 6. Note that the measured resistance is much closer to the calculation made with 10 elements than the one with only 1 element, which shows the advantage of using a more accurate model.

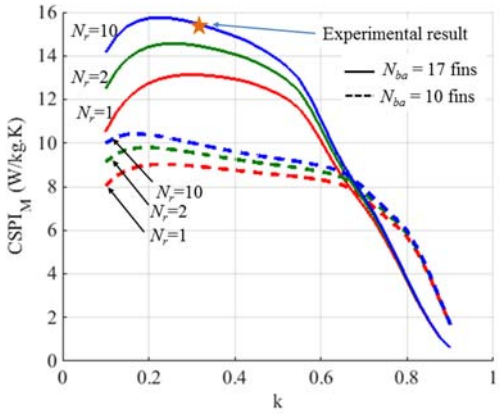

Fig. 5. Calculated heatsink performance index CSPI_M for different fin widths (represented by k), number of fins (N_{ba}) and number of elements (N_r) used to model the heatsink. Measured value in a customized heat sink is marked by a star. Great error in heatsink resistance may exist for thin fins if heat sink is modeled by only one element in the resistance network.

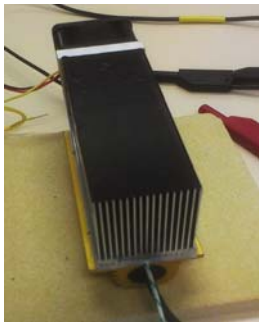

Fig. 6. Manufactured heat sink used to verify the accuracy on thermal resistance model having 10 elements in the resistance network. Weight = 0.286kg and thermal resistance = 0.23K/W.

B. Influence of heat sink length

Heat sink length is usually determined by the size and the number of semiconductors attached to it or by geometrical constraints given by the converter case. Sometimes long heat sinks are needed for multilevel converters, such as in [9], where many switching cells are placed side-by-side. Long heat sinks cause high pressure drop in their air channels, which result on lower heat dissipation performance for a given fan. This is illustrated in Fig. 8 where we show the heat sink performance index $CSPI_M$ for different heat sink length L and for different 40x40mm fans. It has fixed base plate height H_p = 8mm, width and fin height W=H_a=40mm. It is made of aluminum. Each point in the curves is calculated for the optimal value of k and number of fins N_{ba}. We consider that the heat source is homogenously distributed in the heat sink base plate. As said before, the influence of the base plate for small surface heat source will be addressed in future work.

Note in Fig. 8 that the difference between the curves for short heat sinks (low values of l) is mainly due to the fan weight, which is high when compared to the aluminum weight. It is interesting to observe that there is a maximum value of the performance index for each fan. For heat sink longer than the optimal one, the heat sink pressure drop in so high that the fan cannot efficiently blow the air through fins. That is why more powerful fans have optimal $CSPI_M$ for longer heat sinks.

Regarding Fig. 8, one can say that, for commercial axial fans, lengths maximizing the heat dissipation are between 60 and 120% of the heat sink width and height.

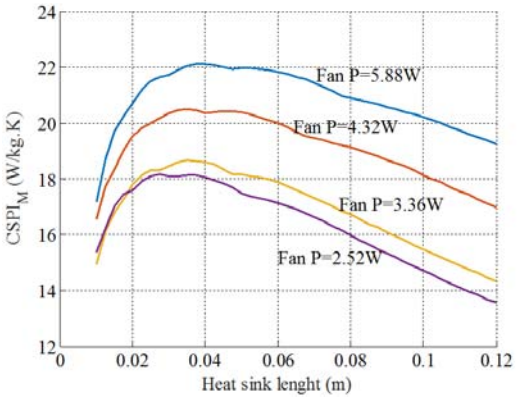

Fig. 7. Calculated heatsink performance index $CSPI_M$ for different aluminum heatsink lengths and different 40x40mm fans. Curves are shown for optimal k and number of fins. High length values cause high pressure drop in the heatsink channels which reduces the heat extraction capability. $CSPI_M$ is low for short heat sinks due to the fan weight.

C. Influence of heat sink height and width

Heat sink width is usually determined by the size and the number of semiconductors attached to the base plate. Fin height depends mainly on the heat sink width since most of fans have squared front surface (examples: 40x40mm, 80x80mm, 120x120mm…). However there is an optimal ratio between fin height and heat sink width (H_a/W) which minimizes the performance index.

This is illustrated in Fig. 9 where we show the variation of $CSPI_M$ with the ratio H_a/W. For the curves 1 and 2, the fan surface is fixed to 80mmx80mm=6400mm² and the fan characteristic used for all the points in the curve corresponds to fan Sanyo Denki 9GA0824P2S001 (fan power 10.1W), although theoretically this fan could not be used in a heat sink having H_a/W different from 1. The heat sink has fixed length L=10mm, base plate height at curves 1 and 2 are, respectively, 8 and 30mm and is made of aluminum. Each point in the curves is calculated for the optimal value of k and number of fins N_{ba}.

In curve 3, the heat sink width is fixed to 80mm and the different number of fans is used. The reference fan is a 40x40mm Sanyo Denki 9GA0412P3J01 (having a power ¼ of the one used in curves 1 and 2). $CSPI_M$ is calculated for four different fin heights: 40mm (using 2 side-by-side fans), 80mm (using 2 rows of 2 side-by-side fans), 120mm (using 3 rows of 2 side-by-side fans) and 160mm (using 4 rows of 2 side-by-side fans). These points correspond to, respectively, H_a/W= 0.5, 1, 1.5 and 2.

Curve 2 shows that wide heat sinks (i.e. for low values of H_a/W) have a significant weight (i.e. low $CSPI_M$) given that the base plate is high and its weight is proportional to the heat sink width. High values of H_a/W also have low values of $CSPI_M$ given that the heat on the base plate cannot achieve the high parts of high thin fins. Thus, there is a fin height value which optimizes the performance index on curve 2. However, in curve 1, since the base plate is short, its influence in the total weight is minimal and thus the higher the fins height, the lower the performance index.

In a system with fixed base plate, an optimal cooling system solution regarding weight is to use small fans and short fins. In the example shown in curve 3, a solution with fin height equal to half the value of the heat sink width (and using 1 row of 2 side-by-side fans) is the one presenting the best performance index.

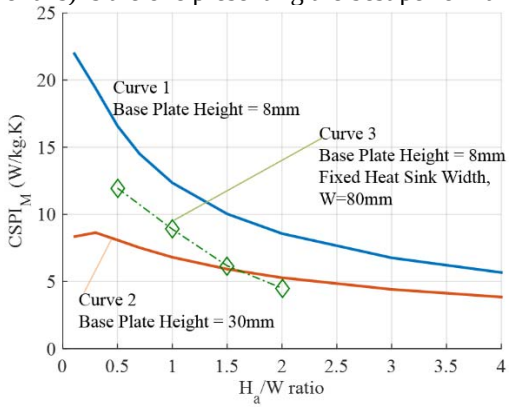

Fig. 8. Calculated aluminum heatsink performance index $CSPI_M$ for different height/width ratios. Curve 1 and 2 have no fixed width but fixed front surface (6400mm²), fixed fan characteristic and base plate height of 8 and 30mm respectively. Curve 3 has fixed base plate and different fin heights having different number of rows containing 2 side-by-side fans. Optimal cooling system for this fixed base plate configuration has 1 row of 2 side-by-side fans (fin height is half the base plate width).

D. Influence of heat sink material

Heat sink in power converters are usually made of extruded aluminum given the interesting manufacturing price. However different materials can be used. In [8], authors compare the performance of sub-optimal heat sinks made of aluminum and copper. They show that, for the same heat sink volume and fan, an optimized copper heat sink has about 18% lower thermal resistance than that made of aluminum. However, in aerospace applications where weight is the main parameter to be reduced, copper heat sinks may not be the best options, as it will be shown below.

Comparison between heat sink materials will be performed regarding the performance index $CSPI_M$ defined above. Besides copper and aluminum, also heat sink made of natural graphite will be considered given the fact that this technology is now well known and several manufacturers produce graphite heat sinks, although the price of such technology is more than 10 times higher than that of aluminum. Thermal conductivity and specific weight of these three materials are shown in Table II. Note that aluminum and copper have isotropic thermal conductivity while the graphite conductivity shown in Table II is valid in only one dimension; in the other two dimensions conductivity is around 57 times lower.

TABLE II. PROPERTIES OF THERMAL MATERIALS [10]

Thermal Material	***Thermal Conductivity (W/mK)***	***Specific Weight (kg/m^3)***
Aluminum	210	2700
Copper	380	8930
Natural Graphite	370	1940

Table II shows that copper has almost twice the thermal conductivity of aluminum, and thus it can more efficiently transport heat through the fins allowing thinner fins to be designed. However, since copper is more than 3 times more dense than aluminum, copper heat sinks are usually heavier than aluminum heat sink. A better material for heat sinks is graphite, which has about the same conductivity of copper and has lower mass density than aluminum.

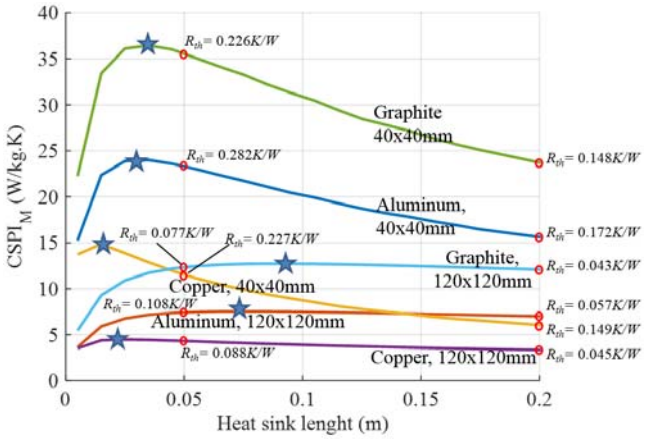

Fig. 9. Calculated heatsink performance index $CSPI_M$ for different heatsink lengths, materials and front sizes: *Case 1* - 40x40mm (using 1 fan); *Case 2* - 120x120mm (using 3 rows of 3 side-by-side fans). Curves are shown for optimal k and number of fins. Aluminum heat sinks have higher performance index than copper ones. Graphite have the highest performance index but it is around 10 times more expensive than aluminum. Maximum performance index for each case is marked with a star and the thermal resistance for some points are marked with circles. Note that each considered heat sink is entirely made of a unique material.

Comparison of optimal heat sinks made with these materials is illustrated in Fig. 10 where we show the heat sink performance index $CSPI_M$ for different heat sink lengths. It has fixed base plate height H_p = 8mm. Width and fin height are either 40x40mm of 120x120mm. In the first case, one Sanyo Denki 9GA0412P3J01 fan (power 5.9W) is used and in the second case 9 of the same fan is used (3 rows of 3 side-by-side fans), to maintain the same air flow. Each point in the curves is calculated for the optimal value of k and number of fins. Note in Fig. 10 that curves for each case show that graphite is the material which attains the highest performance index. For example, taking the curves for a 40x40mm case, the $CSPI_M$ at the optimal length for the graphite is 50% higher than that of aluminum and 140% times higher than that of copper. Also note that, although the total weight of heat sink of case 2 (120x120mm) has lower influence of base plate than that of case 1, case 2 has higher fins which have lower efficiency on heat conduction. Finally, note that, even if heat sink thermal resistance decreases with heat sink length, the weight increases faster. That is why heat sinks with larger dimensions have lower performance indexes.

IV. Conclusions

Aerospace applications require power converter weight minimization. Cooling represents a great part of the system weight and optimization is then essential for a good converter design. This paper explains the optimization of a cooling system composed of an extruded heat sink attached to a fan. We defined a performance index based on cooling system global thermal resistance and mass. The variation of this performance index with the fan characteristics and heat sink dimensions and material was performed.

Results demonstrate that cooling systems with short heat sinks have poor performance index given the fixed weight of the fan. Also long heat sinks result on poor performance index given the great pressure drop in the air channel which reduces the fan capacity to blow air. There is then an optimal heat sink length to maximize the performance index, which depends on the fan characteristic. In the same manner, performance index depends on the ratio between height and width of a heat sink. Wide heat sinks have low performance index given the great influence of base plate on the total weight. Low performance is also observed for high heat sinks known that heat is not efficiently transferred to the fins.

Optimization concerning different materials shows that copper heat sinks are more compact than then ones made of aluminum although they are heavier. Heat sinks using graphite achieve the highest performance index although they could be more than 10 more expensive than aluminum heat sinks.

References

[1] U. Badstuebner, J. Biela, D. Christen, J. W. Kolar, "Optimization of a 5-kW Telecom Phase-Shift DC–DC Converter With Magnetically Integrated Current Doubler," IEEE Trans. Industrial Electronics, vol. 58, n. 10, pp. 4736-4745, Oct. 2011.

[2] K. Raggl, T. Nussbaumer, G. Doerig, J. Biela, J. W. Kolar, "Comprehensive Design and Optimization of a High-Power-Density Single-Phase Boost PFC," IEEE Trans. Industrial Electronics, vol. 56, n. 7, pp. 2574-2587, July 2009.

[3] J. Brandelero, "Conception et réalisation d'un convertisseur multicellulaire DC/DC isolé pour application aéronautique", PhD Dissertation, INPT, Toulouse, France 2015.

[4] M. Holahan, "Fins, fans, and form: volumetric limits to air-side heat sink performance," Inters. Conf. on Thermal and Thermomechanical Phenomena in Electronic Systems (ITHERM), pp. 564,570, Jun 2004.

[5] R. Simons, "Estimating Parallel Plate-Fin Heat Sink Thermal Resistance," Electronics Cooling, Feb. 2003.

[6] P. Teertstra, M. Yovanovich, J. Culham, T. Lemczyk, "Analytical forced convection modeling of plate fin heat sinks," IEEE semiconductor Thermal Measurement and Management Symp., pp. 34-41, Mar 1999.

[7] Puqi Ning, G. Lei, F. Wang, K.D.T. Ngo, "Selection of heatsink and fan for high-temperature power modules under weight constraint," IEEE Applied Power Electr. Conf. and Expo. (APEC), pp.192-198, Feb. 2008.

[8] U. Drofenik, J. W. Kolar, "Sub-Optimum Design of a Forced Air Cooled Heat Sink for Simple Manufacturing," Power Conversion Conference (PCC), Nagoya, Japan, April 2007.

[9] N. Videau, et al., "5-phase interleaved buck converter with gallium nitride transistors," IEEE Workshop on Wide Bandgap Power Devices and Applications (WiPDA), pp.190-193, Oct. 2013.

[10] Zweben, "Revolutionary new thermal management materials," Electron. Cooling, vol. 11, n. 2, pp. 36–37, May 2005.